Renormalization of the NN interaction with Lorentz-invariant chiral two-pion exchange

R. Higa,[1,2,*] M. Pavón Valderrama,[3,4,†] and E. Ruiz Arriola[3,‡]
[1]*Universität Bonn, HISKP (Theorie), Nussallee 14-16, D-53115 Bonn, Germany*
[2]*Jefferson Laboratory, 12000 Jefferson Avenue, Newport News, VA 23606, USA*
[3]*Departamento de Física Atómica, Molecular y Nuclear, Universidad de Granada, E-18071 Granada, Spain*
[4]*H. Niewodniczański Institute of Nuclear Physics, PL-31342 Kraków, Poland*
(Received 5 June 2007; revised manuscript received 19 September 2007; published 25 March 2008)

The renormalization of the NN interaction with the chiral two-pion exchange potential computed using Lorentz-invariant baryon chiral perturbation theory is considered. The short distance singularity reduces the number of counterterms to about half those in the heavy baryon expansion. Phase shifts and deuteron properties are evaluated with clear improvements in some cases.

DOI: 10.1103/PhysRevC.77.034003 PACS number(s): 13.75.Cs, 03.65.Nk, 11.10.Gh, 21.30.Fe

I. INTRODUCTION

At long distances, the nucleon-nucleon (NN) interaction can be written as (see, e.g., Ref. [1] for a review)

$$\mathbf{V}(r) = \mathbf{V}_{1\pi}(r) + \mathbf{V}_{2\pi}(r) + \cdots, \tag{1}$$

where $\mathbf{V}_{1\pi}(r)$ and $\mathbf{V}_{2\pi}(r)$ represent the one-pion exchange (OPE) and the two-pion exchange (TPE) contributions to the potential, respectively. Up to power corrections in the distance r, one has $\mathbf{V}_{n\pi}(r) = \mathcal{O}(e^{-nm_\pi r})$. Such an expansion makes sense, since there is a clear scale separation at long distances. Actually, the omitted terms in Eq. (1) represent contributions whose ranges are shorter than $1/(2m_\pi) \sim 0.7$ fm. These include three-pion and higher exchanges, correlated meson exchanges, etc. [2]. In momentum space, the expansion of Eq. (1) parallels an expansion on leading low-momentum singularities, rather than a naive low-momentum expansion. The systematic and model-independent determination of those potentials was suggested several years ago [3–6] and pursued by many others, see Refs. [7–11] (for some reviews emphasizing different viewpoints, see, e.g., Refs. [12–16] and references therein). However, in any scheme, the potentials in Eq. (1) become singular at short distances, so one must truncate or renormalize the potential in a physically meaningful way in order to predict finite and unique phase shifts and deuteron properties. This has been a subject of much debate and controversy in recent times, and we refer the interested reader to the literature for further details [10,17–31].

In previous works by two of us (M.P.V. and E.R.A.) [25,26,28,29], the renormalization of NN potentials was studied using chiral potentials based on the heavy baryon formalism (HB-χPT) [8,10]. In the present paper, we extend those ideas to the case where Lorentz-invariant chiral potentials are used instead. In this case, the relativistic framework of baryon chiral perturbation theory (RB-χPT) proposed by Becher and Leutwyler [32,33] is employed in the construction of the two-pion exchange (TPE) component of the NN interaction. The remarkable difference between HB- and RB-TPE potentials lies in the long distance behavior [34–37], because of the analytic structure of the πN scattering amplitude in the low-energy region where the Mandelstam variable t is close to $4m_\pi^2$, m_π being the pion mass. Actually, one appealing feature of the RB-TPE potentials is that the long-distance two-pion effects are correctly described, so that important contributions at the exponential level $\sim e^{-2m_\pi r}$ are properly resummed, unlike its heavy baryon counterpart. In this work, we are also interested on its different short distance behavior, which plays an important role in the renormalization program of the NN interaction developed in Refs. [25,26,28,29]. We disregard, however, explicit Δ's (see, e.g., Ref. [38]) and other intermediate state contributions, assuming that those degrees of freedom have been integrated out.

As we have already mentioned, the calculation of scattering and bound state properties requires specifying the NN potential at short distances, which turns out to be highly singular for the Lorentz-invariant case. Actually, a crucial issue in the present context regards the number of necessary counterterms required by the renormalizability of the S matrix. In the single-channel situation, the results found in Refs. [25,26,28,29] in configuration space can be summarized as follows. If the potential is a regular one, i.e., $r^2|U(r)| < \infty$, there is freedom to *choose* between the regular and irregular solution of the corresponding Schrödinger equation. In the first case, the scattering length is predicted, while in the second case, the scattering length becomes an input of the calculation. Singular potentials fulfill $r^2|U(r)| \to \infty$ and do not allow this choice. For repulsive singular potentials [$r^2U(r) \to \infty$], the scattering length is *predicted*; while for attractive singular potentials [$r^2U(r) \to -\infty$], the scattering length *must* be given. The case $r^2U(r) \to g$ is very special and for $g < -1/4$, yields ultraviolet limit cycles [22,39,40]. For coupled channels, one must diagonalize first the coupled-channel potentials and apply the single-channel rules to the outgoing eigenpotentials.

To avoid any possible misunderstanding, we hasten to emphasize that our use of the word "relativistic" is in a narrow sense; we are only disregarding a naive heavy baryon expansion of the virtual nucleon states in the calculation of the potential and hence taking into account important anomalous

*higa@itkp.uni-bonn.de
†mpavon@ugr.es
‡earriola@ugr.es

threshold singularities [32,33]. This is *not the same* as providing a fully relativistic quantum field theoretical solution to the the two-body problem by, say, solving a Bethe-Salpeter equation or any two-body relativistic equation. This has always been a problem rooted in the nonperturbative divorce between crossing and unitarity in few-body calculations for which the present paper has nothing to say.

The paper is organized as follows. In Sec. II we give an overview of our formalism already used in Refs. [25,26,28,29]. The key aspects on the derivation of the Lorentz-invariant TPE potential are briefly mentioned, and the main differences with respect to the heavy baryon formalism are highlighted in Sec. III. The deuteron bound state is discussed in Sec. IV. Our predictions for phase shifts are displayed in Sec. V. Finally, in Sec. VI we draw our conclusions.

II. FORMALISM

Along the lines of Refs. [25,26,28,29], we solve the coupled-channel Schrödinger equation in configuration space for the relative motion, which in compact notation reads

$$-\mathbf{u}''(r)+\left[\mathbf{U}(r)+\frac{\mathbf{l}^2}{r^2}\right]\mathbf{u}(r)=k^2\mathbf{u}(r). \tag{2}$$

The coupled-channel matrix reduced potential is defined as usual, $\mathbf{U}(r)=2\mu_{np}\mathbf{V}(\mathbf{r})$, where $\mu_{np}=M_pM_n/(M_p+M_n)$ is the reduced proton-neutron mass. For $j>0$, $\mathbf{U}(r)$ can be written as

$$\begin{aligned}\mathbf{U}^{0j}(r)&=U^{0j}_{jj},\\ \mathbf{U}^{1j}(r)&=\begin{pmatrix}U^{1j}_{j-1,j-1}(r) & 0 & U^{1j}_{j-1,j+1}(r)\\ 0 & U^{1j}_{jj}(r) & 0\\ U^{1j}_{j-1,j+1}(r) & 0 & U^{1j}_{j+1,j+1}(r)\end{pmatrix}.\end{aligned} \tag{3}$$

In Eq. (2), $\mathbf{l}^2=\mathrm{diag}(l_1(l_1+1),\ldots,l_N(l_N+1))$ is the angular momentum, $\mathbf{u}(r)$ is the reduced matrix wave function, and k the c.m. momentum. In our case, $N=1$ for the spin singlet channel ($l=j$), and $N=3$ for the spin triplet channel, with $l_1=j-1$, $l_2=j$, and $l_3=j+1$. The potentials used in this paper were obtained in Refs. [34–36], in coordinate space. We outline the main issues of this potential in Sec. III.

A. Long distance behavior

At long distances, we assume the usual asymptotic normalization condition

$$\mathbf{u}(r)\to\hat{\mathbf{h}}^{(-)}(r)-\hat{\mathbf{h}}^{(+)}(r)\mathbf{S}, \tag{4}$$

with $\mathbf{S}$ the coupled-channel unitary S matrix. The corresponding outgoing and incoming free spherical waves are given by

$$\hat{\mathbf{h}}^{(\pm)}(r)=\mathrm{diag}\left(\hat{h}^{\pm}_{l_1}(kr),\ldots,\hat{h}^{\pm}_{l_N}(kr)\right), \tag{5}$$

with $\hat{h}^{\pm}_l(x)$ the reduced Hankel functions of order l, $\hat{h}^{\pm}_l(x)=xH^{\pm}_{l+1/2}(x)$ [$\hat{h}^{\pm}_0(x)=e^{\pm ix}$], and satisfy the free Schrödinger's equation for a free particle.

The spin singlet state ($s=0$) is an uncoupled state

$$S^{0j}_{jj}=e^{2i\delta^{0j}_j}, \tag{6}$$

while the spin triplet state ($s=1$) comprises one uncoupled $l=j$ state

$$S^{1j}_{jj}=e^{2i\delta^{1j}_j}, \tag{7}$$

and the two channel coupled $l,l'=j\pm1$ states, for which we use the Stapp-Ypsilantis-Metropolis (SYM or Nuclear bar) [41] parametrization

$$\begin{aligned}S^{1j}&=\begin{pmatrix}S^{1j}_{j-1\,j-1} & S^{1j}_{j-1\,j+1}\\ S^{1j}_{j+1\,j-1} & S^{1j}_{j+1\,j+1}\end{pmatrix}\\ &=\begin{pmatrix}\cos(2\bar{\epsilon}_j)e^{2i\bar{\delta}^{1j}_{j-1}} & i\sin(2\bar{\epsilon}_j)e^{i(\bar{\delta}^{1j}_{j-1}+\bar{\delta}^{1j}_{j+1})}\\ i\sin(2\bar{\epsilon}_j)e^{i(\bar{\delta}^{1j}_{j-1}+\bar{\delta}^{1j}_{j+1})} & \cos(2\bar{\epsilon}_j)e^{2i\bar{\delta}^{1j}_{j+1}}\end{pmatrix}.\end{aligned}$$

In the present paper, zero energy scattering parameters play an essential role, since they are often used (see below) as input parameters in the calculation of phase shifts. Due to the unitarity of the S matrix in the low-energy limit $k\to0$, we have

$$(\mathbf{S}-\mathbf{1})_{l',l}=-2i\alpha_{l',l}k^{l'+l+1}+\cdots, \tag{8}$$

with $\alpha_{l'l}$ the (Hermitian) scattering length matrix. The threshold behavior of the SYM phases is

$$\bar{\delta}^{1j}_{j-1}\to-\bar{\alpha}^{1j}_{j-1}k^{2j-1}, \tag{9}$$

$$\bar{\delta}^{1j}_{j+1}\to-\bar{\alpha}^{1j}_{j+1}k^{2j+3}, \tag{10}$$

$$\bar{\epsilon}_j\to-\bar{\alpha}^{1j}_{j}k^{2j+1}. \tag{11}$$

B. Short distance behavior

The form of the wave functions at the origin is uniquely determined by the form of the potential at short distances (see, e.g., Refs. [42,43] for the case of one channel and Refs. [25,26,28,29] for coupled channels). For the Lorentz-invariant chiral NN potential , one has

$$\mathbf{U}_{2\pi}(r)\to\frac{M\mathbf{C}_7}{r^7},$$

which resembles a relativistic Van der Waals force (see, e.g., Ref. [44] for the electromagnetic case). Note that this short distance behavior without an $1/M$ expansion is at variance with the nonrelativistic $1/r^5$ and $1/r^6$ in the standard Weinberg counting based on the HB chiral expansion. In the latter, the expansion around the limit $M\to\infty$ is built in the formalism, leading to a different behavior at $r\to0$.

For a potential diverging at the origin as an inverse power law, one has

$$\mathbf{U}(r)\to\frac{M\mathbf{C}_n}{r^n}, \tag{12}$$

with $\mathbf{C}_n$ a matrix of generalized Van der Waals coefficients and $n>2$. One diagonalizes the matrix $\mathbf{C}_n$ by a constant unitary transformation $\mathbf{G}$, yielding

$$M\mathbf{C}_n=\mathbf{G}\,\mathrm{diag}\left(\pm R_1^{n-2},\ldots,\pm R_N^{n-2}\right)\mathbf{G}^{-1}, \tag{13}$$

with R_i constants with length dimension. The plus sign corresponds to the case with a positive eigenvalue (attractive) and the minus sign to the case of a negative eigenvalue (repulsive). Then, at short distances, one has the solutions

$$\mathbf{u}(r) \to \mathbf{G} \begin{pmatrix} u_{1,\pm}(r) \\ \cdots \\ u_{N,\pm}(r) \end{pmatrix}, \tag{14}$$

where for the attractive and repulsive cases, one has

$$u_{i,-}(r) \to C_{i,-} \left(\frac{r}{R_i}\right)^{n/4} \sin\left[\frac{2}{n-2}\left(\frac{R_i}{r}\right)^{\frac{n}{2}-1} + \varphi_i\right], \tag{15}$$

$$u_{i,+}(r) \to C_{i,+} \left(\frac{r}{R_i}\right)^{n/4} \exp\left[-\frac{2}{n-2}\left(\frac{R_i}{r}\right)^{\frac{n}{2}-1}\right], \tag{16}$$

respectively. Here, φ_i are arbitrary short distance phases which in general depend on the energy. There are as many short distance phases as short distance attractive eigenpotentials. Orthogonality of the wave functions at the origin yields the relation

$$\sum_{i=1}^{N} [u_{k,i}{}^* u'_{p,i} - u'_{k,i}{}^* u_{p,i}]|_{r=0} = \sum_{i=1}^{A} \cos(\varphi_i(k) - \varphi_i(p)), \tag{17}$$

where $A \leqslant N$ is the number of the short distance attractive eigenpotentials. Details on the numerical implementation of these short distance boundary conditions can be found in Refs. [25,26,28,29].

C. Numerical parameters

The Lorentz-invariant chiral TPE potential is specified by the pion weak decay constant f_π, the nucleon axial coupling constant g_A, the nucleon mass M_N, and the pion mass m_π. In addition, at the level of approximation that we are working, it is enough to consider the low-energy constants c_1, c_3, and c_4 which characterize πN scattering. The corresponding RB potential is specified by the same parameters at N^{3}LO in the HB chiral expansion.

In our numerical calculations, one takes $f_\pi = 92.4$ MeV, $m_\pi = 138.03$ MeV, $2\mu_{np} = M_N = 2M_pM_n/(M_p + M_n) = 938.918$ MeV, $g_A = 1.29$ in the OPE piece to account for the Goldberger-Treimann discrepancy and $g_A = 1.26$ in the TPE piece of the potential. The corresponding pion-nucleon coupling constant takes then the value $g_{\pi NN} = 13.083$, according to the Nijmegen phase-shift analysis of NN scattering [45]. The values of the coefficients c_1, c_3, and c_4 used in this paper can be found in Table I, which lists several sets that have been proposed in the literature [10,20,46,47] as well as the one that will be used in the present work based on our analysis of deuteron properties below.

Renormalization requires fixing some low-energy parameters while removing the cutoff. We take the values from the high-quality potentials [48,49] as have been obtained in Ref. [50] for the NijmII and Reid93 versions. We will use the Nijm II values for definiteness. As mentioned earlier, the number of independent parameters or counterterms requires a study of the attractive/repulsive nature of the potential at short distances. The result of such an analysis for all channels considered in this work is summarized in Table II for the different parameter sets. We also list the scattering lengths in all partial waves with $j \leqslant 5$ as determined in our previous work [50].

TABLE I. Sets of chiral coefficients (in GeV^{-1}) considered in this work.

Set	Source	c_1	c_3	c_4
I	πN [46]	−0.81	−4.69	3.40
II	NN [10]	−0.76	−5.08	4.70
III	NN [47]	−0.81	−3.40	3.40
IV	NN [20]	−0.81	−3.20	5.40
η	This work	−0.81	−3.80	4.50

III. LORENTZ-INVARIANT TWO-PION EXCHANGE

A series of papers [34–37] is devoted to the construction of the TPE component of the NN interaction, based on the Lorentz-invariant formulation of baryon chiral perturbation theory proposed by Becher and Leutwyler [32,33] in their study of the πN system. Becher and Leutwyler showed that it is possible to obtain a consistent power counting in a theory with a heavy particle without resorting to an integration, at the Lagrangian level, of its heavy degrees of freedom, and subsequent expansion around the limit of infinitely heavy baryon (HB-χPT). For completeness we briefly review such an approach here. The so-called infrared regularization separates, for a certain loop integral $I_{\rm full}$, all the soft ($I_{\rm IR}$) and the hard ($R_{\rm IR}$) virtual modes in a Lorentz-invariant way. The former retains all the low-energy analytic structures dictated by chiral symmetry. The latter has a complicated analytic structure only high energies—its low-energy expansion amounts to a simple Taylor series in the generic low-momenta p over the heavy scales in the system[1] ($\Lambda_\chi \sim 4\pi f_\pi \sim m_\rho$ or M_N). This term is the one responsible for violating the power counting in the (Lorentz-invariant) baryon sector and can be absorbed by suitable counterterms in a chiral-invariant way. For a deeper understanding of the concepts and technical details, we refer the reader to Refs. [32,51–54].

In principle, the $I_{\rm IR}$ part, when expanded in powers of p/M_N, reproduces the HB results. However, this expansion is not always allowed, since it destroys the correct analytic behavior of the amplitude near the low-energy region close to $t = 4m_\pi^2$. The underlying reason comes from the anomalous threshold of the triangle graph [32] (Fig. 1) right below threshold, $t = 4m_\pi^2 - m_\pi^4/M_N^2$. In the heavy baryon limit, this singularity is ignored (as it collapses to the normal threshold) and any $1/M_N$ expansion of the triangle loop around this region will fail to converge. Note that the same triangle integral also appears in the TPE potential, with two pseudovector vertices

[1] Within this scheme, it is possible to verify that nucleon loops, antinucleons, etc., contribute only to the $R_{\rm IR}$ term.

TABLE II. Number of independent parameters (counterterms) for the Lorentz-invariant baryon expansion potential (RB) and different orders of approximation of the heavy baryon expansion (HB) potential. The scattering lengths are in $\mathrm{fm}^{l+l'+1}$ and are taken from NijmII and Reid93 potentials [48] in Ref. [50]. We use the (SYM-nuclear bar) convention, Eq. (11). The stars (*) mean that the behavior is very dependent on the chosen set of chiral couplings.

Wave	α NijmII (Reid93)	OPE	HB-NLO	HB-NNLO Sets I, II, & III	HB-NNLO Set IV	RB-TPE
$^1S_0$	−23.727(−23.735)	Input	Input	Input	Input	Input
$^3P_0$	−2.468(−2.469)	Input	–	Input	–	–(*)
$^1P_1$	2.797(2.736)	–	–	Input	–	–
$^3P_1$	1.529(1.530)	–	Input	Input	Input	Input
$^3S_1$	5.418(5.422)	Input	–	Input	Input	Input
$^3D_1$	6.505(6.453)	–	–	Input	Input	–
E_1	1.647(1.645)	–	–	Input	Input	–
$^1D_2$	−1.389(−1.377)	–	Input	Input	Input	Input
$^3D_2$	−7.405(−7.411)	Input	Input	Input	Input	Input
$^3P_2$	−0.2844(−0.2892)	Input	Input	Input	Input	Input
$^3F_2$	−0.9763(−0.9698)	–	–	Input	–	–(*)
E_2	1.609(1.600)	–	–	Input	–	–(*)
$^1F_3$	8.383(8.365)	–	–	Input	–	Input
$^3F_3$	2.703(2.686)	–	Input	Input	Input	Input
$^3D_3$	−0.1449(−0.1770)	Input	–	Input	Input	Input
$^3G_3$	4.880(4.874)	–	–	Input	Input	–
E_3	−9.695(−9.683)	–	–	Input	Input	–
$^1G_4$	−3.229(−3.210)	–	Input	Input	Input	Input
$^3G_4$	−19.17(−19.14)	Input	Input	Input	Input	Input
$^3F_4$	−0.01045(−0.01053)	Input	Input	Input	Input	Input
$^3H_4$	−1.250(−1.240)	–	–	Input	–	–(*)
E_4	3.609(3.586)	–	–	Input	–	–(*)
$^1H_5$	28.61(28.57)	–	–	Input	–	Input
$^3H_5$	6.128(6.082)	–	Input	Input	Input	Input
$^3G_5$	−0.0090(−0.010)	Input	–	Input	Input	Input
$^3I_5$	10.68(10.66)	–	–	Input	Input	–
E_5	−31.34(−31.29)	–	–	Input	Input	–

in one nucleon and a Weinberg-Tomozawa seagull term in the other.

To illustrate the problem, let us consider the spectral representation of the triangle graph,

$$\gamma(t) = \frac{1}{\pi}\int_{4m_\pi^2}^{\infty} \frac{dt'}{(t'-t)}\,\mathrm{Im}\gamma(t'), \tag{18}$$

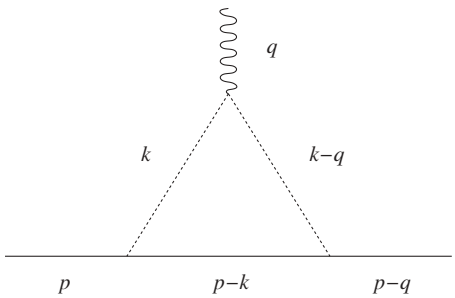

FIG. 1. Triangle diagram, which cannot be reproduced by the usual heavy baryon expansion close to $t = 4m_\pi^2$. The solid, dashed, and wiggly lines represent, respectively, the nucleon, the pions, and an external scalar source.

where

$$\mathrm{Im}\gamma(t') = \frac{\theta\left(t'-4m_\pi^2\right)}{16\pi M_N\sqrt{t'}}\,\arctan\frac{2M_N\sqrt{t'-4m_\pi^2}}{t'-2m_\pi^2}. \tag{19}$$

In HB-χPT, the argument $x = 2M_N\sqrt{t'-4m_\pi^2}/(t'-2m_\pi^2)$ is assumed to be of order q^{-1}, yielding the expansion $\arctan x = \pi/2 - 1/x + 1/3x^3 + \cdots$. The first two terms read

$$\begin{aligned}\gamma(-q^2)|_{\mathrm{HB}} &= \frac{1}{16\pi^2 M_N m_\pi}\int_{4m_\pi^2}^{\infty}\frac{dt'}{(t'+q^2)} \\ &\quad\times\frac{1}{\sqrt{t'}}\left[\frac{\pi}{2} - \frac{\left(t'-2m_\pi^2\right)}{2M_N\sqrt{t'-4m_\pi^2}}\right] \\ &= \frac{1}{16\pi^2 M_N m_\pi}\left[2\pi m_\pi A(q)\right. \\ &\quad\left.+\frac{m_\pi}{M_N}\frac{\left(2m_\pi^2+q^2\right)}{\left(4m_\pi^2+q^2\right)}L(q)\right],\end{aligned} \tag{20}$$

where $q = |\boldsymbol{q}|$, and $L(q)$ and $A(q)$ are the usual HB loop functions

$$L(q) = \frac{\sqrt{4m_\pi^2 + q^2}}{q} \ln \frac{\sqrt{4m_\pi^2 + q^2} + q}{2m_\pi},$$
$$A(q) = \frac{1}{2q} \arctan \frac{q}{2m_\pi}. \tag{21}$$

However, it does not take into consideration the case $|x| < 1$, when t' gets closer to $4m_\pi^2$. This region, where the naive heavy baryon expansion fails, is responsible for the long distance behavior of the triangle diagram, as can be seen by its representation in configuration space,

$$\Gamma(r) = \frac{1}{\pi} \int_{4m_\pi^2}^{\infty} dt' \int \frac{d^3q}{(2\pi)^3} e^{-i\boldsymbol{q}\cdot\boldsymbol{r}} \frac{\mathrm{Im}\gamma(t')}{t' + q^2}$$
$$= \frac{1}{4\pi^2} \int_{4m_\pi^2}^{\infty} dt' \frac{e^{-r\sqrt{t'}}}{r} \mathrm{Im}\gamma(t'). \tag{22}$$

The equation above clearly shows that to have a good asymptotic description of $\Gamma(r)$, one needs a decent representation for $\mathrm{Im}\gamma(t')$ near $t' = 4m_\pi^2$. This is only possible if one takes the triangle anomalous threshold into account, which cannot be provided by current versions of the heavy baryon formalism.

The potential in configuration space is obtained through a Fourier transform of the potential in momentum space. There, one faces the problem of nonlocalities, i.e., terms dependent on the variable $z = p + p'$, where p and p' are the initial and final c.m. momenta of the NN system. The Lorentz-invariant loop integrals, which incorporate the dynamics of the TPE, also depend on this variable in a nontrivial way. However, phenomenologically one learns that such terms are not relevant at low energies, and a Taylor expansion in z is usually considered.[2] In this case, the Fourier transform can be carried out in an easier way (see, for instance, Refs. [55,56]). Generically, in any spin-isospin channel and up to the considered order in the RB expansion, the potentials may be written as a function of at most second order in the total momentum operator. In this paper, we take the local approximation on the radial part of the potentials and keep only up to linear terms in the operators. The remaining nonlocalities are fairly small all over the range of interest, which somehow justifies its exclusion and considerably simplifies our calculations.[3]

[2]For instance, in the heavy baryon potential, nonlocalities show up only at $O(q^4)$ ($\mathrm{N^3LO}$).

[3]A rough way of estimating this in coordinate space is by acting with the operator ∇^2/m_π^2 on the local function that multiplies the variable z^2 and comparing with the local that multiplies the variable z^0. In the region between 0.01 and 2 fm, these functions behave indeed as $1/r^7$ and are not parametrically small, but the ratio between the nonlocal and local contribution is at the level of 1–5%.

IV. THE DEUTERON

In the proton-neutron (pn) c.m. system, the deuteron wave function is

$$\Psi(\vec{x}) = \frac{1}{\sqrt{4\pi}r} \left[u(r)\sigma_p \cdot \sigma_n + \frac{w(r)}{\sqrt{8}} (3\sigma_p \cdot \hat{x}\sigma_n \cdot \hat{x} - \sigma_p \cdot \sigma_n) \right] \chi_{pn}^{sm_s}, \tag{23}$$

with the total spin $s = 1$ and $m_s = 0, \pm 1$, and σ_p and σ_n the Pauli matrices for the proton and the neutron, respectively. The functions $u(r)$ and $w(r)$ are the reduced S- and D-wave components of the relative wave function, respectively. They satisfy the coupled set of equations in the ${}^3S_1$-${}^3D_1$ channel

$$-u''(r) + U_{{}^3S_1}(r)u(r) + U_{E_1}(r)w(r) = -\gamma^2 u(r),$$
$$-w''(r) + U_{E_1}(r)u(r) + \left[U_{{}^3D_1}(r) + \frac{6}{r^2} \right] w(r) = -\gamma^2 w(r), \tag{24}$$

with $U_{{}^3S_1}(r)$, $U_{E_1}(r)$, and $U_{{}^3D_1}(r)$ the corresponding matrix elements of the coupled-channel potential. We solve Eq. (24) together with the asymptotic condition at infinity

$$u(r) \to A_S e^{-\gamma r},$$
$$w(r) \to A_D e^{-\gamma r} \left(1 + \frac{3}{\gamma r} + \frac{3}{(\gamma r)^2} \right), \tag{25}$$

where $\gamma = \sqrt{MB}$ is the deuteron wave number (B is the deuteron binding energy), A_S is the s-wave normalization factor determined from the condition

$$\int_0^\infty dr[u(r)^2 + w(r)^2] = 1, \tag{26}$$

and the asymptotic D/S ratio parameter is defined by $\eta = A_D/A_S$. As we have already mentioned, the RB-TPE potential displays a $1/r^7$ singularity (similar to the relativistic Van der Waals) at the origin. Thus, the discussion of whether the deuteron parameters γ and η can be fixed independently of the potential depends on the short distance behavior of the eigenvalues of the coupled-channel potential matrix. As discussed in Refs. [25,26,28,29] also for the bound state case, the number of independent parameters coincides with the number of negative (attractive) eigenpotentials at short distances. In the RB-TPE potential we are using here [34–36], we have only one independent parameter (see Table II) which we take to be γ or, equivalently, the deuteron binding energy. With such a choice, η becomes a prediction in contrast to the HB-TPE, where η is an input. The outgoing deuteron wave functions are depicted in Fig. 2 for the RB-TPE potential and compared to the HB-TPE one.

Let us analyze in more detail the cutoff dependence of observables in the present RB-TPE potential. Given the fact that in the ${}^3S_1$-${}^3D_1$ coupled channel we have one attractive and one repulsive eigenpotential at short distances, we may borrow from the previous discussion on OPE [25], to which we refer the reader for further details. The practical way of introducing in this case a short distance cutoff r_c which selects the regular solution at the origin is by appropriately choosing the auxiliary boundary condition at the point $r = r_c$ among

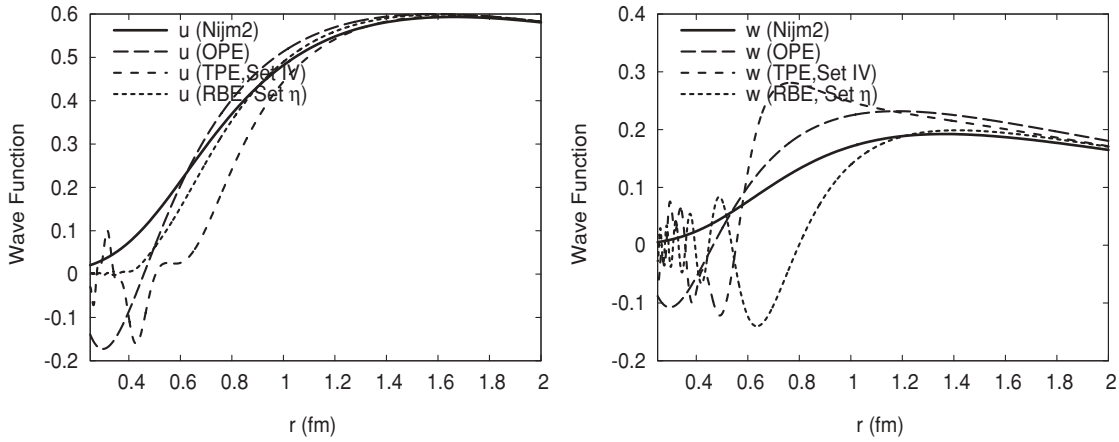

FIG. 2. RB-TPE deuteron wave functions, u (left) and w (right), as functions of distance r compared with the HB-TPE and Nijmegen II wave functions [48]. The asymptotic normalization $u \to e^{-\gamma r}$ has been adopted, and the asymptotic D/S ratio is taken $\eta = 0.0256(4)$ in the TPE case (for OPE, $\eta = 0.026333$). We use set IV of chiral couplings and set η (see Table I).

many possible choices compatible with self-adjointness [25]. The precise choice may provide smoother limits and hence better convergence properties in the pre-asymptotic region. Actually, as we show in the Appendix, we can estimate the size of the finite cutoff corrections in deuteron observables and hence their convergence rate toward the corresponding renormalized values. The result is that up to some oscillations the convergence toward the renormalized value is exponential as $r_c \to 0$, i.e., the convergence toward the renormalized value is $\eta(r_c) - \eta(0) \sim \exp[-4/5(R_+/r_c)^{\frac{5}{2}}]$ for the RB-TPE potential ($\sim 1/r^7$) as compared to $\eta(r_c) - \eta(0) \sim \exp[-2(R_+/r_c)^{\frac{1}{2}}]$ for the OPE potential ($\sim 1/r^3$). Here R_+ is a characteristic short distance scale of the corresponding repulsive eigenpotentials. The analysis of the Appendix also shows that, generally, the more singular the potential the faster the convergence.

For illustration purposes, we show in Fig. 3 the calculated asymptotic D/S ratio of the deuteron wave function η as a function of the short distance cutoff r_c (in fm) for the RB-TPE potential when the auxiliary boundary conditions $u(r_c) = 0$ and $u'(r_c) = 0$ are considered. Note the clear and coincident plateau below $r_c = 0.4$ fm for both boundary conditions following a relatively rapid variation above this region.[4] As mentioned above, this is a typical feature of a coupled-channel singular potential with one attractive and one repulsive eigenpotential which extends to all other deuteron properties. Actually, the situation strongly resembles the previously studied OPE potential which has a softer $1/r^3$ singularity at the origin [25]; the main difference is that for OPE, stability takes place at a shorter scale, $r_c = 0.2$ fm, than in RB-TPE potential. In the present context, it is also helpful to remember that a short distance cutoff radius and a sharp momentum cutoff are inversely proportional to each other, $r_c = \pi/(2\Lambda)$ [57] (the numerical coefficient depends on the particular regularization). Thus plotting observables as a function of r_c enhances the finite cutoff changes, while long plateaus could be observed instead as functions of Λ. Actually, halving the short distance cutoff corresponds to doubling the momentum space cutoff. For instance, in RB (set η) the range $r_c = 0.3$–0.4 fm corresponds to the range $\Lambda = 780$–1030 MeV, where observables such as η change less than 0.01%. Pinning down this error bar would be harder if the sharp or other momentum space cutoff was used.

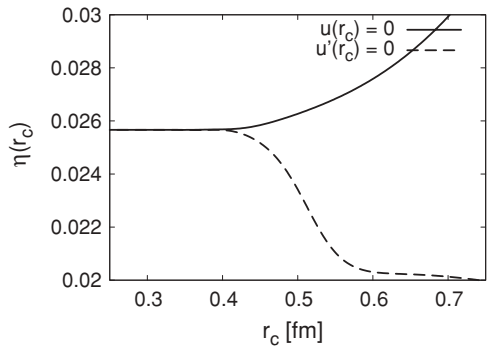

FIG. 3. Cutoff dependence of the asymptotic D/S ratio of the deuteron wave function η as a function of the short distance cutoff r_c for the RB-TPE potential for the auxiliary boundary conditions $u(r_c) = 0$ and $u'(r_c) = 0$. We use set η of chiral couplings (see Table I) designed to reproduce the experimental value $\eta = 0.0256(4)$ in the limit $r_c \to 0$. The convergence toward the renormalized value is $\eta(r_c) - \eta(0) \sim \exp[-2/5(R_+/r_c)^{\frac{5}{2}}]$ up to oscillations (see main text).

Our results for several deuteron properties are shown in Table III and compared with the corresponding HB-TPE considered in our previous work [25,26,28,29]. Some remarks concerning the errors quoted in Table III are in order. We provide the largest source of error in the calculation which we are able to quantify. Since we aim at renormalized results, we stop whenever the change of the cutoff causes no significant variation within a prescribed accuracy, which we take to be about an order of magnitude higher than the typical

[4]Other auxiliary boundary conditions such as $w(r_c) = 0$ or $w'(r_c) = 0$ not shown in the figure make the oscillations deduced in the Appendix more visible, but the plateau region takes place also below $r_c = 0.4$ fm and yields an identical numerical result as with $u(r_c) = 0$ and $u'(r_c) = 0$.

TABLE III. Deuteron properties for the OPE and the HB-TPE and RB-TPE potentials. We use the nonrelativistic relation $\gamma = \sqrt{2\mu_{np}B}$ with $B = 2.224575(9)$. The errors in the OPE case are estimated by changing the short distance cutoff in the range 0.1–0.2 fm. The errors quoted in the HB-TPE reflect the uncertainty in only the nonpotential parameters γ, η. The errors quoted in the RB-TPE are estimated as in the OPE case, but changing the cutoff in the range 0.3–0.4 fm. The entry Exp. stands for experimental and/or recommended values and can be traced from Ref. [58].

Set	γ(fm^{-1})	η	A_S(fm$^{-1/2}$)	r_d(fm)	Q_d(fm^2)	P_D	$\langle r^{-1}\rangle$(fm^{-1})	$\langle r^{-2}\rangle$(fm^{-2})	$\langle r^{-3}\rangle$(fm^{-3})
OPE	Input	0.02634	0.8681(1)	1.9351(5)	0.2762(1)	7.88(1)%	0.4861(10)	0.434(3)	∞
HB set IV	Input	Input	0.884(4)	1.967(6)	0.276(3)	8(1)%	0.447(5)	0.284(8)	0.276(13)
RBE set IV	Input	0.03198(3)	0.8226(5)	1.8526(10)	0.3087(2)	22.99(13)%	0.5054(15)	0.360(4)	0.333(13)
RBE set η	Input	0.02566(1)	0.88426(2)	1.96776(1)	0.2749(1)	5.59(1)%	0.4438(3)	0.2714(7)	0.215(3)
NijmII	0.231605	0.02521	0.8845(8)	1.9675	0.2707	5.635%	0.4502	0.2868	∞
Reid93	0.231605	0.02514	0.8845(8)	1.9686	0.2703	5.699%	0.4515	0.2924	∞
Exp.	0.231605	0.0256(4)	0.8846(9)	1.971(6)	0.2859(3)	5.67(4)%	–	–	–

experimental or recommended value uncertainty. Thus, the cutoff range is not necessarily the same in all cases. In general terms, the more singular the potential at short distance, the faster the convergence of the result toward the renormalized limit (see, e.g., the Appendix). Thus, the toughest case is OPE, where we only have $1/r^3$ singularity. Convergence in this case is the slowest, therefore shorter cutoffs $r_c = 0.1$–0.2 fm are needed.

The value we obtain for η for the parameter sets of Table I is slightly different from the experimental one, making the comparison with the HB-TPE case [26], where η was a free parameter (two attractive short distance eigenpotentials), a bit misleading. To obtain an accurate value of η it was necessary to readjust the low-energy parameters c_3 and c_4 to the values $c_3 = -3.8$ and $c_4 = 4.5$ GeV^{-1}, indeed, very similar to the values proposed by other authors [10,20,46,47] (see Table I). Actually, once we have reproduced η we see a general and slight improvement in accuracy when going from the HB-TPE (where η is a free parameter) of our previous work [26] to the present RB-TPE calculation (where η is predicted). Basically, RB-TPE produces a sharp prediction for η (with eventually no errors), whereas HB-TPE does not predict η, so its 1% experimental uncertainty propagates to other deuteron observables at about a similar 1% level, which is still comparable to or larger than the error in the quoted experimental or recommended values. The conclusion in Ref. [26] was that agreement was partly achieved because of this fuzziness in the theoretical predictions. Of course, one should not over stress the possible accuracy of the present results as regards the systematic errors; the main point of our calculation is to provide the general picture when more complete asymptotic TPE effects are correctly taken into account.

V. PHASE SHIFTS

We come to the calculation of the neutron-proton (np) phase shifts. In practice, this requires a careful wave-by-wave study of the renormalized limit. As can be seen in Table II, all coupled triplet channels have one attractive and one repulsive short distance $1/r^7$ eigenpotential. On the other hand, almost all singlet and uncoupled triplet channels develop an attractive $1/r^7$ singularity at short distances (sometimes depending on the parameter values). The only exceptions we found are the $^1P_1$ and $^3P_0$ channels, the latter depending on the precise values of the $c_{1,3,4}$ constants of the chiral potential. This fact determines not only the number of counterterms, but also the convergence pattern toward the renormalized result. It reaches stability for cutoffs ranging in the region $r_c = 0.3$–0.5 fm, depending on the particular partial wave and also on the energy (see the discussion in Sec. IV and the Appendix).

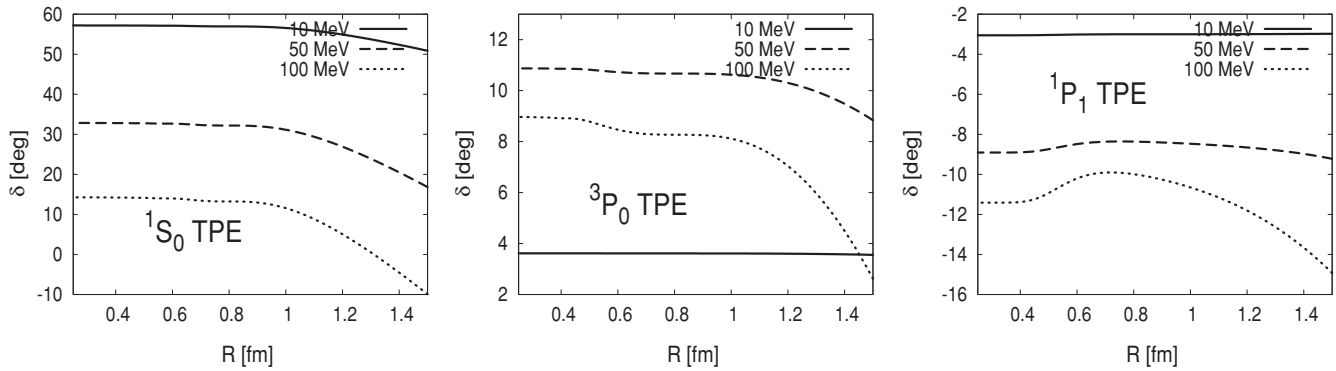

FIG. 4. RBE np phase shifts in the $^1S_0$, $^3P_0$, and $^1P_1$ channels as functions of the short distance cutoff radius R for the fixed laboratory energies $T_L = 10, 50, 100$ MeV.

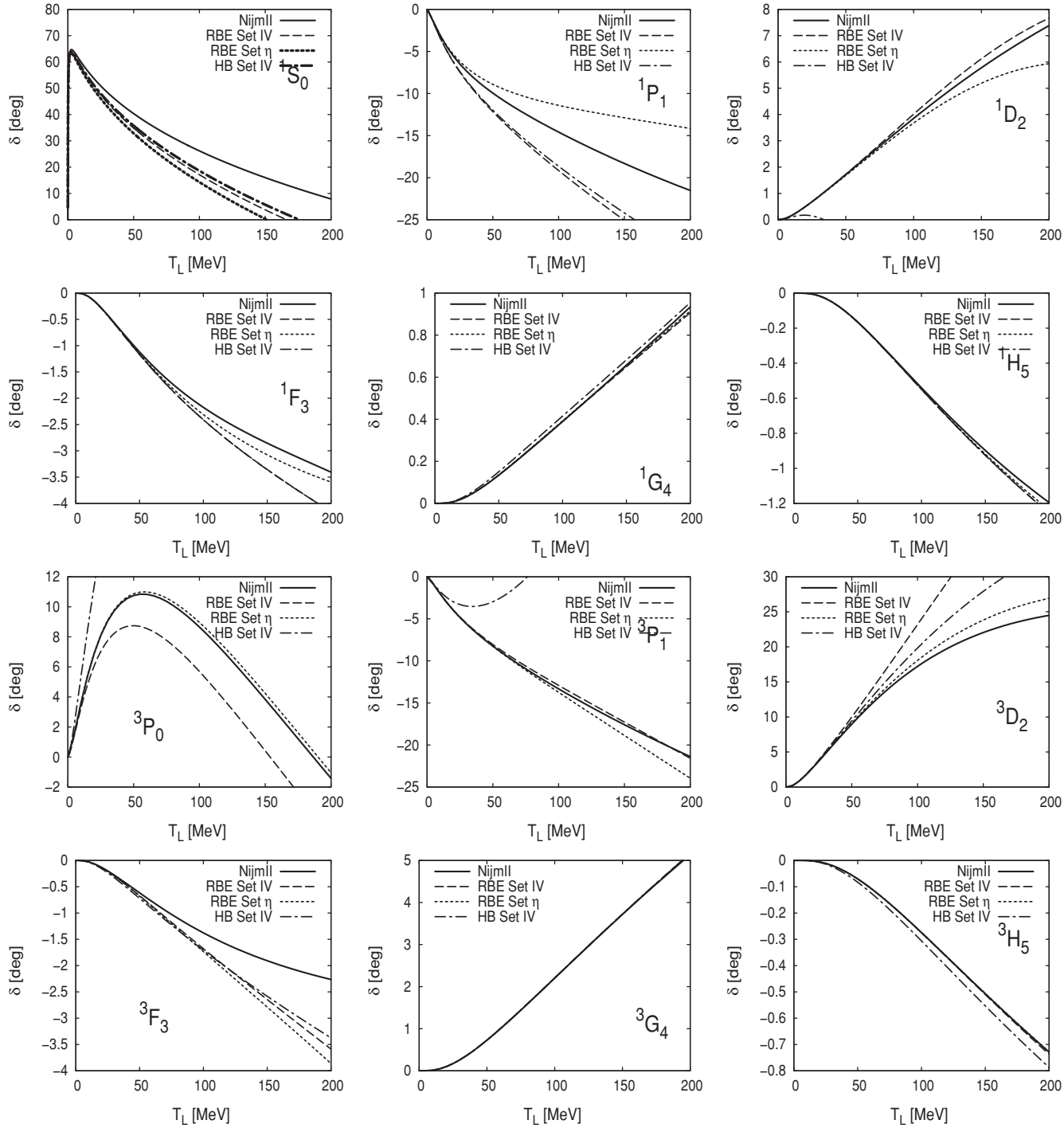

FIG. 5. np (SYM-nuclear bar) spin singlet and uncoupled spin triplet phase shifts for the total angular momentum $j = 0, 1, 2, 3, 4, 5$ for RBE and HBE as a function of the laboratory energy compared with the Nijmegen partial-wave analysis [48,49].

Phase shifts in coupled channels with one repulsive singular component have been computed with either of the auxiliary boundary conditions $u_{0,j,l=j-1}(r_c) = 0$ or $u'_{0,j,l=j-1}(r_c) = 0$ for zero energy states and subsequent orthogonalization of the finite energy states by using a complementary boundary condition as described in detail in Ref. [25] for the OPE case. It is important to realize that even though renormalization in principle requires one to pursue the mathematical limit $r_c \to 0$, and that this limit indeed fixes the number of independent parameters, convergence is achieved in practice by length scales which are not unrealistically small and in fact are rather reasonable. Actually, the stability plateaus take place around the previous HB cutoffs but above the nucleon Compton wavelength $1/M_N \sim 0.2$ fm, which shows that after renormalization, the value of the phase shift is not determined by the relativistic-like $1/r^7$ singularity. This can be seen

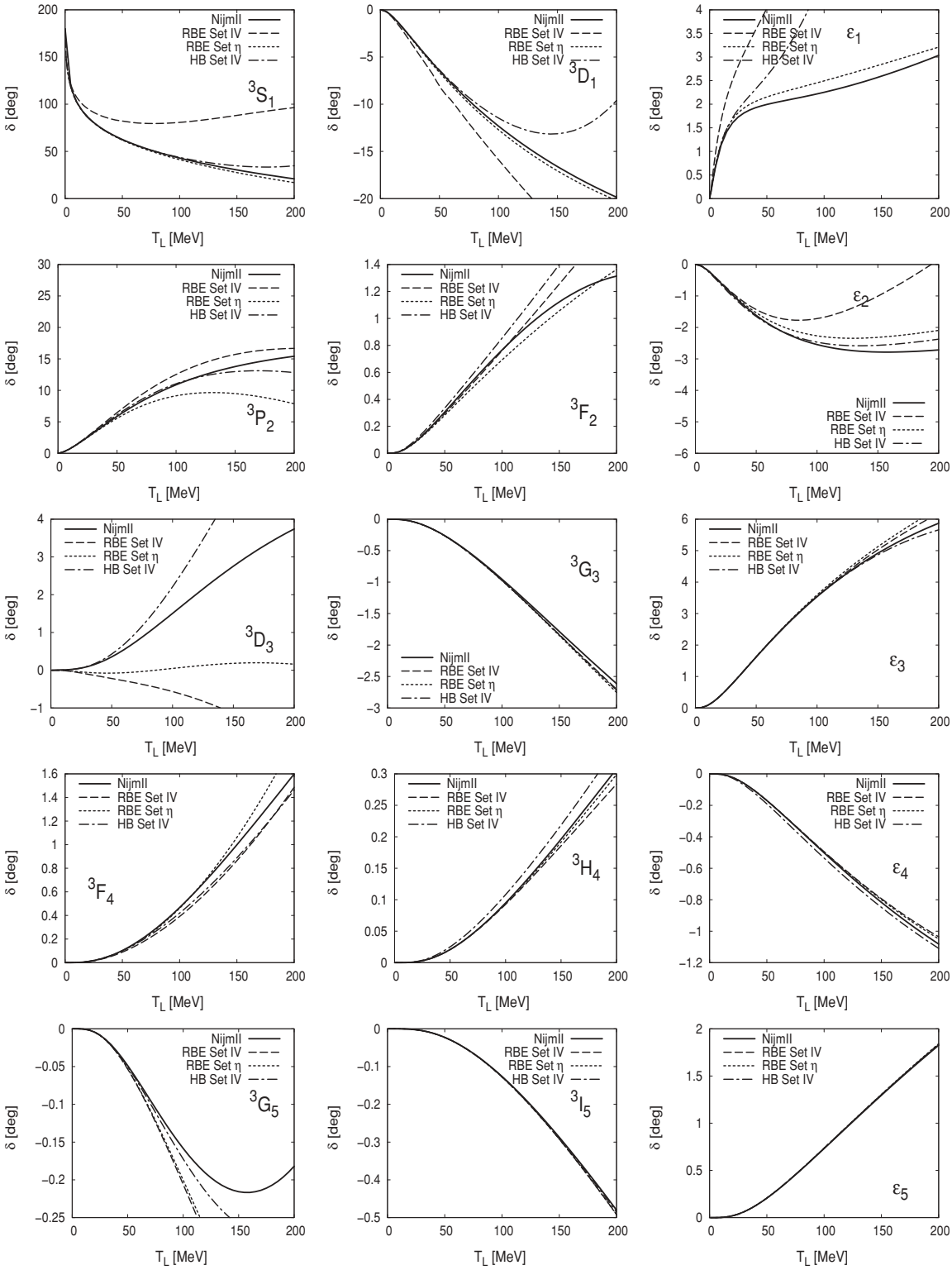

FIG. 6. Same as Fig. 5, but for coupled spin triplet phase shifts.

in Fig. 4, which depicts, for purposes of illustration, some selected low phases as functions of the short distance cutoff for fixed laboratory energy values. As one generally expects, smaller values of r_c are needed as the energy is increased. The approach toward the renormalized value for any partial wave depends on the attractive/repulsive character of the singular potential at short distances. So, the $^1S_0$ and $^3P_0$ channels are purely attractive, and hence the finite cutoff corrections are $\mathcal{O}(r_c^{\frac{7}{2}+1})$ up to oscillations [40]. On the other hand, the $^1P_1$ channel provides a repulsive case, and hence finite cutoff

corrections are $\mathcal{O}[\exp(-r_c^{-\frac{5}{2}})]$. We recall that the smallest de Broglie wavelength probed in NN interaction below the pion production threshold is $\lambda \sim 0.5$ fm. Thus, the RB potential and the present renormalization construction also implement the desirable *a priori* requirement that short distance details are indeed irrelevant for the description of low-energy properties.

In Figs. 5 and 6, we present the np (SYM-nuclear bar) renormalized phase shifts for the total angular momentum $j = 0, 1, 2, 3, 4, 5$ for spin singlet and uncoupled spin triplet and for coupled spin triplet channels, respectively. There, we compare the relativistic baryon expansion (RBE) and the heavy baryon expansion (HBE) as a function of the laboratory energy compared with the Nijmegen partial-wave analysis [48,49]. For definiteness, we use the chiral constants c_1, c_3, and c_4 of Ref. [20] (set IV), which already provided a good description of deuteron properties after renormalization [26] at next-to-next-to-leading order (NNLO). This choice allows a more straightforward comparison to the N^{3}LO calculation of Ref. [20] with finite cutoffs. We also compare with the set η which takes the same value of c_1 and the readjusted values $c_3 = -3.8$ and $c_4 = 4.5$ GeV^{-1} based on our improved description of the deuteron in Sec. IV. Unless otherwise stated, the needed low-energy parameters for these figures are *always* taken to be those of Ref. [50] for the NijmII potential (see Table II). As can be clearly seen, the RB-TPE with this set η improves not only the deuteron properties but also the phase shifts all over with the notable exception of the $^3D_3$. Again, one should not overemphasize this agreement, but it is rewarding to see that there is a general trend to stability and improvement in some channels (such as $^1D_2$, $^3P_1$, and $^3P_0$) when the RB-TPE potential is considered, while the quality of description is not worsened in other channels. At the same time, however, one should stress that generally speaking, this potential needs fewer counterterms than the corresponding HB counterpart (about a half). Actually, in the Lorentz-invariant potential case, one has at most one parameter per channel instead of the three parameters channel in the coupled triplets for the heavy-baryon case. This is because of the attractive-repulsive short distance character of the coupled-channel RB-TPE as compared to the attractive-attractive HB-TPE potential in these coupled channels. Again, we recall that the RB-TPE provides the correct analytic behavior of the exchange of two pions at large distances when Δ and other excitations are not explicitly considered.

VI. CONCLUSIONS

In the present paper, we have analyzed the renormalization of all partial waves with $j \leqslant 5$ for NN scattering and the bound deuteron state for the chiral two-pion exchange potential computed in a Lorentz-invariant baryon expansion. Our main motivation has been to consider a potential where the asymptotic TPE effects are consistently taken care of. This gives us some confidence that long distance physics is more faithfully represented by a common exponential falloff factor $e^{-2m_\pi r}$. At the level of calculation considered here, Δ and other excitations are not explicitly taken into account; within a Lorentz-invariant baryon expansion, the contribution of this degree of freedom to the NN potential has never been computed. As we have repeatedly stressed throughout this paper, this Lorentz-invariant potential presents a $1/r^7$ singularity at the origin, which demands renormalization in order to obtain a finite and unique result when the TPE potential is assumed to be valid all over the range from the origin to infinity. This can be done by introducing a number of (potential independent) counterterms, and consequently physical renormalization conditions must be specified. In practice they are fixed to the values of threshold parameters, mainly scattering lengths at zero energy. Actually, we have noted that the number of necessary counterterms is drastically reduced when the Lorentz-invariant baryon potential is compared to the heavy baryon expanded TPE potential, while both potentials are specified by the same parameters. Thus, less input is needed to predict the NN phase shifts. Although the precise number of counterterms depends on the parameters of the potential, we find that typically for the channels with total angular momentum $j = 0$–5, we need 13 in the Lorentz-invariant case as compared to about 27 in the HB potential. Actually, it is noteworthy that with about half the number of counterterms, the overall agreement is improved. This is particularly striking in the $^3P_0$ and $^3S_1$-$^3D_1$ (deuteron) channels. In other channels, the improvement is moderate, indicating missing shorter range contributions to Eq. (1). Although a deeper understanding of why this dramatic reduction of the number of counterterms happens would very helpful, and we have not attempted a large scale fit, it is very rewarding that the implementation of the correct and fairly complete long range physics deduced from one- and two-pion exchange in conjunction with the requirement of renormalizability provides a rather reasonable description of the NN scattering data below the pion production threshold.

ACKNOWLEDGMENTS

We would like to thank the hospitality of the European Center for Theoretical Studies on Nuclear Physics and Related Areas (ECT*) in Trento, where this work was initiated. M.P.V. also thanks W. Broniowski and P. Bożek for their kind hospitality in Krakow where part of this work was carried out. The work of M.P.V. and E.R.A. is supported in part by the Spanish DGI and FEDER with Grant no. FIS2005-00810, Junta de Andalucía Grant no. FQM225-05, and EU Integrated Infrastructure Initiative Hadron Physics Project Contract no. RII3-CT-2004-506078. The work of R.H. was supported by DOE Contract no. DE-AC05-06OR23177, under which SURA operates the Thomas Jefferson National Accelerator Facility, and by the BMBF under Contract no. 06BN411.

APPENDIX: ANALYTICAL DETERMINATION OF FINITE CUTOFF CORRECTIONS

In this Appendix, we determine the finite cutoff corrections to renormalized deuteron properties when the the two coupled-channel potential is such that there is one attractive and one repulsive short distance eigenpotential. This is the case of the OPE and RB-TPE potentials discussed in this paper. In this

case, it is simplest to discuss the auxiliary boundary condition

$$u(r_c) = 0. \tag{A1}$$

The analysis of other auxiliary boundary conditions such as $u'(r_c) = 0$, which has actually been used in the numerical calculations, is a bit messier; but the final conclusion is essentially the same as with Eq. (A1).

From the superposition principle of boundary conditions, we may write

$$\begin{aligned} u(r) &= u_S(r) + \eta u_D(r), \\ w(r) &= w_S(r) + \eta w_D(r), \end{aligned} \tag{A2}$$

where $(u_S(r), w_S(r))$ and $(u_D(r), w_D(r))$ solve the deuteron problem in Eq. (24) with the long distance boundary conditions of Eq. (25) when taking $(A_S, A_D) = (1, 0)$ and $(A_S, A_D) = (0, 1)$, respectively. On the other hand, at short distances, the coupled-channel potential is diagonalized by an orthogonal transformation

$$\mathbf{G} = \begin{pmatrix} \cos\theta & \sin\theta \\ -\sin\theta & \cos\theta \end{pmatrix}, \tag{A3}$$

where the mixing angle θ depends on the parameters of the potential only. For instance, for OPE, one has $\cos\theta = -1/\sqrt{3}$, see Ref. [25]. The reduced potential behaves as

$$\mathbf{U}(r) \to \frac{1}{r^n}\mathbf{G}\begin{pmatrix} +R_+^{n-2} & 0 \\ 0 & -R_-^{n-2} \end{pmatrix}\mathbf{G}^{-1}, \tag{A4}$$

where R_+ and R_- are the Van der Waals length scales associated with the repulsive and attractive channels, respectively. Defining the general short distance solutions of the decoupled problems, we have

$$\begin{aligned} v_{i,+}(r) &= \left(\frac{r}{R_+}\right)^{n/4}\left\{a_{i,+}\exp\left[-\frac{2}{n-2}\left(\frac{R_+}{r}\right)^{\frac{n-2}{2}}\right]\right. \\ &\quad \left. + b_{i,+}\exp\left[+\frac{2}{n-2}\left(\frac{R_+}{r}\right)^{\frac{n-2}{2}}\right]\right\} \\ v_{i,-}(r) &= \left(\frac{r}{R_-}\right)^{n/4} c_{i,-}\sin\left[\frac{2}{n-2}\left(\frac{R_-}{r}\right)^{\frac{n-2}{2}} + \varphi_i\right], \end{aligned} \tag{A5}$$

where $i = S, D$ and $a_{i,+}$, $b_{i,+}$, $c_{i,-}$, and φ_i are fixed constants that depend on the potential only and may be determined by integrating in from long distances the asymptotic wave functions $(u_S(r), w_S(r))$ and $(u_D(r), w_D(r))$. We recall that $n = 7$ for the RB-TPE potential, while $n = 3$ for the OPE potential. Note that we must include here also the diverging exponential at the origin for the repulsive eigenpotential. The solutions at short distances behave as

$$\begin{pmatrix} u_i(r) \\ w_i(r) \end{pmatrix} \to \begin{pmatrix} \cos\theta & \sin\theta \\ -\sin\theta & \cos\theta \end{pmatrix}\begin{pmatrix} v_{i,+}(r) \\ v_{i,-}(r) \end{pmatrix}, \tag{A6}$$

where $i = S, D$. Thus, using the short distance boundary condition of Eq. (A1), which selects the regular solution at the origin and eventually kills the diverging exponentials when $r_c \to 0$, and gathering all subsequent equations, we get

$$\begin{aligned} \eta(r_c) &= -\frac{u_S(r_c)}{u_D(r_c)} \\ &\to \frac{\cos\theta v_{S,+}(r_c) + \sin\theta v_{S,-}(r_c)}{\cos\theta v_{D,+}(r_c) + \sin\theta v_{D,-}(r_c)}. \end{aligned} \tag{A7}$$

The limiting value is controlled by the short distance diverging exponentials in Eq. (A5) and is given by

$$\eta(0) = -\frac{b_{S,+}}{b_{D,+}}. \tag{A8}$$

Deviations from this value for small cutoffs r_c can be directly determined from Eq. (A5) yielding

$$\begin{aligned} \frac{\eta(r_c)}{\eta(0)} &= 1 + \tan\theta\left(\frac{R_+}{R_-}\right)^{\frac{n}{4}}\left[\frac{c_{S,-}}{b_{S,+}} - \frac{c_{D,-}}{b_{D,+}}\right] \\ &\quad \times \exp\left[-\frac{2}{n-2}\left(\frac{R_+}{r_c}\right)^{\frac{n-2}{2}}\right] \\ &\quad \times \sin\left[\frac{2}{n-2}\left(\frac{R_-}{r_c}\right)^{\frac{n-2}{2}} + \varphi_i\right] + \cdots, \end{aligned} \tag{A9}$$

showing that, up to oscillations, finite cutoff corrections in the deuteron are $\mathcal{O}[\exp(-r_c^{-\frac{1}{2}})]$ for OPE and $\mathcal{O}[\exp(-r_c^{-\frac{5}{2}})]$ for RB-TPE. The generalization to other auxiliary boundary conditions and other deuteron properties is straightforward with an identical result in the order of finite cutoff effects.

The case of scattering states is more tedious and will not be discussed in detail here but can also be analyzed with a combination of the coupled-channel formulas of Ref. [40] (see Sec. V of that paper) and the bound state results of the present appendix. Finite cutoff effects for the S matrix scale similarly as in the bound state case; i.e., up to oscillations, they are $\mathcal{O}[\exp(-r_c^{-\frac{1}{2}})]$ for OPE and $\mathcal{O}[\exp(-r_c^{-\frac{5}{2}})]$ for RB-TPE.

[1] G. Brown and A. D. Jackson, *The Nucleon-Nucleon Interaction* (North-Holland, Amsterdam, 1976).
[2] R. Machleidt, K. Holinde, and C. Elster, Phys. Rep. **149**, 1 (1987).
[3] S. Weinberg, Phys. Lett. **B251**, 288 (1990).
[4] C. Ordonez and U. van Kolck, Phys. Lett. **B291**, 459 (1992).
[5] S. Weinberg, Nucl. Phys. **B363**, 3 (1991).
[6] C. Ordonez, L. Ray, and U. van Kolck, Phys. Rev. C **53**, 2086 (1996).
[7] T. A. Rijken and V. G. J. Stoks, Phys. Rev. C **54**, 2851 (1996).
[8] N. Kaiser, R. Brockmann, and W. Weise, Nucl. Phys. **A625**, 758 (1997).
[9] J. L. Friar, Phys. Rev. C **60**, 034002 (1999).
[10] M. C. M. Rentmeester, R. G. E. Timmermans, J. L. Friar, and J. J. de Swart, Phys. Rev. Lett. **82**, 4992 (1999).
[11] D. R. Entem and R. Machleidt, Phys. Rev. C **66**, 014002 (2002).
[12] P. F. Bedaque and U. van Kolck, Annu. Rev. Nucl. Part. Sci. **52**, 339 (2002).
[13] D. R. Phillips, Czech. J. Phys. **52**, B49 (2002).
[14] E. Epelbaum, Prog. Part. Nucl. Phys. **57**, 654 (2006).
[15] M. Rho, nucl-th/0610003.

[16] E. Ruiz Arriola and M. Pavon Valderrama, Nucl. Phys. **A790**, 379 (2007).
[17] E. Epelbaum, W. Gloeckle, and U.-G. Meissner, Nucl. Phys. **A671**, 295 (2000).
[18] D. R. Entem and R. Machleidt, Phys. Lett. **B524**, 93 (2002).
[19] S. R. Beane, P. F. Bedaque, M. J. Savage, and U. van Kolck, Nucl. Phys. **A700**, 377 (2002).
[20] D. R. Entem and R. Machleidt, Phys. Rev. C **68**, 041001(R) (2003).
[21] E. Epelbaum, W. Glockle, and U.-G. Meissner, Nucl. Phys. **A747**, 362 (2005).
[22] M. P. Valderrama and E. R. Arriola, Phys. Rev. C **70**, 044006 (2004).
[23] M. C. Birse and J. A. McGovern, Phys. Rev. C **70**, 054002 (2004).
[24] A. Nogga, R. G. E. Timmermans, and U. van Kolck, Phys. Rev. C **72**, 054006 (2005).
[25] M. P Valderrama and E. R. Arriola, Phys. Rev. C **72**, 054002 (2005).
[26] M. Pavon Valderrama and E. Ruiz Arriola, Phys. Rev. C **74**, 054001 (2006).
[27] M. C. Birse, Phys. Rev. C **74**, 014003 (2006).
[28] M. Pavon Valderrama and E. Ruiz Arriola, Phys. Rev. C **74**, 064004 (2006).
[29] M. Pavon Valderrama and E. Ruiz Arriola, Phys. Rev. C **75**, 059905(E) (2007).
[30] E. Epelbaum and U. G. Meissner, nucl-th/0609037.
[31] M. C. Birse, Phys. Rev. C **76**, 034002 (2007).
[32] T. Becher and H. Leutwyler, Eur. Phys. J. C **9**, 643 (1999).
[33] T. Becher and H. Leutwyler, J. High Energy Phys. 06 (2001) 017.
[34] R. Higa and M. R. Robilotta, Phys. Rev. C **68**, 024004 (2003).
[35] R. Higa, M. R. Robilotta, and C. A. da Rocha, Phys. Rev. C **69**, 034009 (2004).
[36] R. Higa, nucl-th/0411046.
[37] R. Higa, M. R. Robilotta, and C. A. da Rocha, nucl-th/0501076.
[38] N. Kaiser, S. Gerstendorfer, and W. Weise, Nucl. Phys. **A637**, 395 (1998).
[39] S. R. Beane, P. F. Bedaque, L. Childress, A. Kryjevski, J. McGuire, and U. vanKolck, Phys. Rev. A **64**, 042103 (2001).
[40] M. Pavon Valderrama and E. Ruiz Arriola, arXiv:0705.2952 [nucl-th].
[41] H. P. Stapp, T. J. Ypsilantis, and N. Metropolis, Phys. Rev. **105**, 302 (1957).
[42] K. M. Case, Phys. Rev. **80**, 797 (1950).
[43] W. Frank, D. J. Land, and R. M. Spector, Rev. Mod. Phys. **43**, 36 (1971).
[44] G. Feinberg, J. Sucher, and C. K. Au, Phys. Rep. **180**, 83 (1989).
[45] J. J. de Swart, M. C. M. Rentmeester, and R. G. E. Timmermans, PiN Newslett. **13**, 96 (1997).
[46] P. Buettiker and U.-G. Meissner, Nucl. Phys. **A668**, 97 (2000).
[47] E. Epelbaum, W. Gloeckle, and U.-G. Meissner, Eur. Phys. J. A **19**, 401 (2004).
[48] V. G. J. Stoks, R. A. M. Klomp, C. P. F. Terheggen, and J. J. de Swart, Phys. Rev. C **49**, 2950 (1994).
[49] V. G. J. Stoks, R. A. M. Klomp, M. C. M. Rentmeester, and J. J. de Swart, Phys. Rev. C **48**, 792 (1993).
[50] M. P Valderrama and E. R. Arriola, Phys. Rev. C **72**, 044007 (2005).
[51] M. R. Schindler, J. Gegelia, and S. Scherer, Phys. Lett. **B586**, 258 (2004).
[52] J. L. Goity, D. Lehmann, G. Prezeau, and J. Saez, Phys. Lett. **B504**, 21 (2001).
[53] D. Lehmann and G. Prezeau, Phys. Rev. D **65**, 016001 (2001).
[54] P. J. Ellis and H.-B. Tang, Phys. Rev. C **57**, 3356 (1998).
[55] M. H. Partovi and E. L. Lomon, Phys. Rev. D **2**, 1999 (1970).
[56] N. Hoshizaki and S. Machida, Prog. Theor. Phys. **24**, 1325 (1960).
[57] M. Pavon Valderrama and E. Ruiz Arriola, in *NSTAR 2004 Proceedings of the Workshop on the Physics of Excited Nucleons, Grenoble, France, 24–27 March 2004,* edited by J.-P. Bocquet, V. Kuznetsov, and D. Rebreyend (World Scientific, Singapore, 2004).
[58] J. J. de Swart, C. P. F. Terheggen, and V. G. J. Stoks, nucl-th/9509032.